

# Realization of a super waveguide for high-power-density generation and transmission using right- and left-handed transmission-line circuits

Yu Hua Yao,<sup>1</sup> Tie Jun Cui,<sup>1,\*</sup> Qiang Cheng,<sup>1</sup> Ruopeng Liu,<sup>1,2</sup> Da Huang,<sup>1</sup> and David R. Smith<sup>2,†</sup>

<sup>1</sup>*Center for Computational Electromagnetics and the State Key Laboratory of Millimeter Waves, Department of Radio Engineering, Southeast University, Nanjing 210096, People's Republic of China*

<sup>2</sup>*Department of Electrical and Computer Engineering, Duke University, Box 90291, Durham, North Carolina 27708, USA*

(Received 12 February 2007; revised manuscript received 3 May 2007; published 7 September 2007)

In an earlier work [Cheng and Cui, Phys. Rev. B **72**, 113112 (2005)], we have shown theoretically that extremely high power densities can be generated and transmitted in a super waveguide which is filled with homogeneous bilayers of right- and left-handed materials. In this paper, we realize such a super waveguide using right-handed transmission-line (RH TL) and left-handed transmission-line (LH TL) circuits. After a rigorous design of the RH TL-LH TL structure, we observe the generation and transmission of high-power densities in the super circuit waveguide from accurate simulation results. Both lossless and lossy cases have been studied for the LH TL circuit. From the simulation results and the rigorous analysis of energy speeds, we show that high-power flows with opposite directions are excited in the RH TL and LH TL parts of the super waveguide, which form the energy vortices in the waveguide cross section.

DOI: [10.1103/PhysRevE.76.036602](https://doi.org/10.1103/PhysRevE.76.036602)

PACS number(s): 41.20.Jb, 78.20.Ci, 42.25.Bs, 42.25.Gy

## I. INTRODUCTION

Waveguide is a very important component for microwave and optical wave transmission. When a waveguide is filled or partially filled with left-handed material (LHM) which possesses negative permittivity and permeability simultaneously [1], some interesting features have been achieved, such as subwavelength cavity resonators [2], backward guided waves [3], guided modes with imaginary transverse wavenumbers [4], enhancement of evanescent waves in waveguides [5], mode coupling of forward and backward waves [6], and TE/TM guided modes in an air waveguide with LHM cladding [7], etc.

Recently, a super waveguide has been proposed theoretically using a homogeneous bilayer of right-handed material (RHM) and LHM, where both lossless and lossy cases have been considered [8]. It has been shown that extremely high-power densities can be generated by the excitation of a line source and high-power flows can be transmitted along the RHM and LHM regions of the waveguide. Later, the above phenomena were also observed when the waveguide is excited by an electric dipole [9]. How to feed the super waveguide through a small aperture was then investigated in Ref. [10].

In real cases, the natural LHM does not exist and it has to be realized using artificially three-dimensional (3D) periodic structures, such as arrays of split-ring resonators (SRR) and wires (or electric resonant cells) [11,12]. However, there is always a relatively large loss in such an artificial LHM, and hence it is difficult to observe the super-waveguide phenomena in a conventional waveguide which is partially filled with the artificial LHM.

Besides using 3D periodic structures, LHM can also be realized using LC-loaded transmission-line (TL) circuits

[13,14], which possesses relatively small loss and can be easily controlled by adjusting the loaded capacitors and inductors. Hence it is possible to verify the super-waveguide phenomena through the circuit model. In this paper, we will realize such a super waveguide using right-handed transmission-line (RH TL) and left-handed transmission-line (LH TL) circuits. We first give a rigorous design of the RH TL-LH TL circuit waveguides. Then we clearly observe the generation and transmission of high-power densities in the super circuit waveguides from accurate simulation results. We also show that high-power flows with opposite directions are excited in the RH TL and LH TL regions of the waveguide. Hence the net power flowing across the super waveguide is small, which is nearly the same as that flowing across the conventional RH TL waveguide. Rigorous analysis of the energy speeds in the RH TL and LH TL regions is given to validate the above conclusions.

## II. REALIZATION OF SUPER WAVEGUIDE USING RH TL AND LH TL CIRCUITS

In the theoretical study of super waveguide, equal-thickness bilayers of air and LHM are filled in a planar waveguide [8]. In order to obtain the generation and transmission of extremely high-power densities, a small retardation was introduced in the lossless LHM, whose permittivity and permeability are given by [8]

$$\epsilon_1 = -\epsilon_0(1 + \delta), \quad \mu_1 = -\mu_0(1 + \delta), \quad (1)$$

in which  $\epsilon_0$  and  $\mu_0$  are permittivity and permeability of air, and  $\delta$  is a small parameter, either positive or negative, defining the retardation. In such a case, a super waveguide can be achieved [8,9].

Now we design the air and LHM with constitutive parameters defined in Eq. (1) using the LC-loaded TL circuits. Based on the TL theory, the effective air and LHM can be generated from two-dimensional periodic circuit structures

\*tjcui@seu.edu.cn

†drsmith@ee.duke.edu

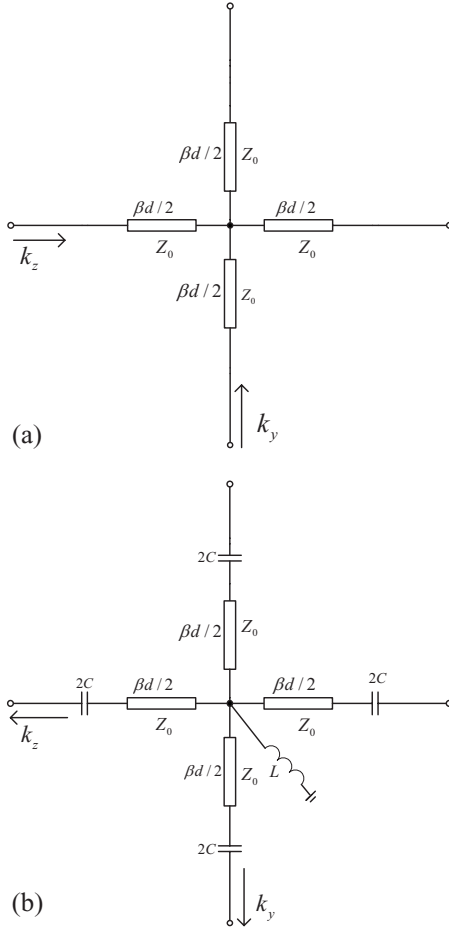


FIG. 1. Unit cells of periodic TL structures. (a) The RHTL mesh. (b) The LHTL mesh.

with unit cells shown in Fig. 1, where the RHTL mesh is used to form air, and the LHTL mesh is used to form LHM [13,14]. In Ref. [14], detailed design formulations of TL circuit parameters shown in Fig. 1 were given to obtain the effective air and LHM

$$Z_0 = \sqrt{2}\eta_0, \quad \beta = \frac{\sqrt{2}}{2}k_0, \quad (2)$$

$$\frac{\cos \frac{1}{2}\beta d}{\omega^2 \mu_0 C d} = \frac{2 + \delta}{1 + \delta}, \quad (3)$$

$$\frac{\cos \frac{1}{2}\beta d}{\omega^2 \epsilon_0 L d} = 2 + \delta, \quad (4)$$

in which  $k_0 = \omega/c_0$  is the wavenumber in air,  $\eta_0 = 120 \pi \Omega$  is the wave impedance in air,  $c_0$  is the light speed in air,  $Z_0, \beta, d$  are the characteristic impedance, propagation constant, and length of the TL section, respectively, and  $L$  and  $C$  are loaded inductance and capacitance. Under such constraints, all circuit parameters  $Z_0, \beta, L$ , and  $C$  are determined once the

frequency  $f$  and the size of unit cell  $d$  are given in real designs.

However, loss is unavoidable in realistic artificial LHM. Hence it is necessary to investigate the power densities within the waveguide when both loss and retardation are involved in LHM. Assume that the permittivity and permeability of LHM are expressed as

$$\epsilon_1 = -\epsilon_0(1 + \delta - i\sigma_\epsilon), \quad \mu_1 = -\mu_0[(1 + \delta) - i\sigma_\mu], \quad (5)$$

where both  $\sigma_\epsilon$  and  $\sigma_\mu$  are small parameters. Using the same method in Ref. [14], the corresponding circuit parameters satisfy the following relations

$$\frac{\cos \frac{1}{2}\beta d}{\omega^2 \mu_0 C d} = \frac{2 + \delta}{1 + \delta} - i\sigma_\mu, \quad (6)$$

$$\frac{\cos \frac{1}{2}\beta d}{\omega^2 \epsilon_0 L d} = 2 + \delta - i\sigma_\epsilon, \quad (7)$$

in which the small imaginary parts in the right-hand sides of Eqs. (6) and (7) result in a small imaginary parts in the capacitance  $C$  and inductance  $L$ , indicating the small resistance.

We have generated a conventional RHTL waveguide and a RHTL-LHTL super waveguide using the LC-loaded TL circuits, as illustrated in Figs. 2(a) and 2(b), respectively. The conventional RHTL waveguide simulates the air-filled waveguide, in which the RHTL mesh shown in Fig. 1(a) extends 36 cells in the  $z$  direction and 180 cells in the  $y$  direction. A voltage source with 1 V (0 dB) is connected to the node of cell numbered as (18, 90) in the RHTL mesh.

For the super waveguide, a total of  $36 \times 180$  unit cells have been used, in which the RHTL and LHTL meshes shown in Figs. 1(a) and 1(b) extend 18 cells in the  $z$  direction, respectively. Both meshes extend 180 cells in the  $y$  direction, as demonstrated in Fig. 2(b). A voltage source with 1 V (0 dB) is placed at the node of cell numbered as (9, 90) in the RHTL region.

In the above configurations, two boundaries in the  $z$  direction are connected to ground to simulate metallic walls. We remark that the ideal waveguides should be infinitely long along the  $y$  direction. In the actual design and simulations, however, the waveguides have to be truncated to finite lengths with proper loads. In our design shown in Fig. 2, we used 180 unit cells along the  $y$  direction, from which we can observe the generation of guided modes by a point voltage source. We further designed a much longer waveguide to study the transmission property of guided waves.

### III. SIMULATIONS AND DISCUSSIONS

In this section, the Agilent's Advanced Design System (ADS) has been used for numerical simulations. We remark that ADS is accurate for LC circuits and LC-loaded transmission lines based on the circuit theory and TL equations, which has been well verified.

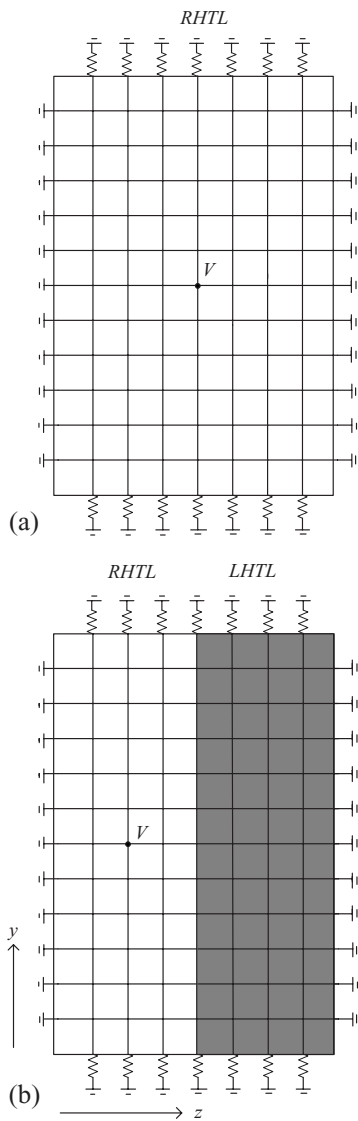


FIG. 2. Realization of the conventional and super waveguides using the RHTL and LHTL circuits. (a) The conventional RHTL waveguide. (b) The RHTL-LHTL super waveguide.

We first consider a case when the driving frequency is set as 1 GHz, the unit size  $d$  is 5 mm, and the retardation parameters are set as  $\delta = -0.0085$  and  $\sigma_\mu = \sigma_\epsilon = 0$ . In such a case, the guidance condition is satisfied [8]. From the design formulations, we easily have  $Z_0 = 533.146 \Omega$  and  $\beta = 14.810$ .

Different terminations along the  $y$  direction will result in different simulation results. If the TL meshes along the  $y$  direction are connected to ground, the two waveguides shown in Fig. 2 become cavities or resonators. In such a situation, the ADS simulation results for the RHTL-LHTL cavity and RHTL-only cavity are demonstrated in Fig. 3. Comparing Figs. 3(a) and 3(b), we clearly see that the voltage amplitudes in two cavities are quite similar, where pure standing waves are observed in both  $y$  and  $z$  directions. In these two figures, only the field patterns around the excitation sources are slightly different. From Fig. 3, we notice that *the high-power density is not generated in the super waveguide cavity* because the waves excited by the source cannot be guided.

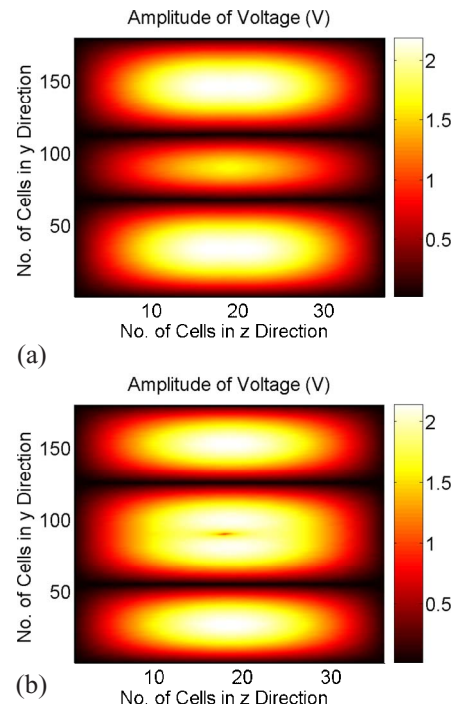


FIG. 3. (Color online) Voltage-amplitude distributions of standing waves in the waveguide cavities (resonators) when  $d = 5$  mm and the TL meshes are ground terminated. (a) The super waveguide cavity with  $\delta = -0.0085$ . (b) The conventional RHTL waveguide cavity.

In order to simulate an infinitely long periodic structure in the  $y$  direction, we use the wave impedance for free space to terminate the TL meshes. Figures 4 and 5 illustrate the ADS simulation results for amplitude distributions of voltage and current density in the RHTL-LHTL super waveguide and conventional RHTL waveguide. From these two figures, we clearly observe that both amplitudes are symmetrically distributed. The maximum amplitudes of voltage and current density in the super waveguide reach 35.7 V and 45.5 mA/m, respectively, which are much larger than those (1.18 V and 1.9 mA/m) in the conventional waveguide. From Figs. 4 and 5, we also notice that the guided waves are actually travelling-standing waves since the load impedance is not matched completely.

The phase distributions of voltage and current density in the RHTL-LHTL super waveguide and the conventional RHTL waveguide are also computed. For the conventional RHTL waveguide, the phase of voltage is symmetrically distributed along both  $y$  and  $z$  directions, and the phase of current density is symmetrically distributed along the  $z$  direction but antisymmetrically distributed ( $180^\circ$  phase shift) along the  $y$  direction, which are not plotted here for space reason. The antisymmetric phase distribution indicates that the current flows upwards above the source point and flows downwards below the source point. For the RHTL-LHTL super waveguide, the phase distributions are illustrated in Fig. 6. Clearly, the phase of voltage is symmetrically distributed along both  $y$  and  $z$  directions, while the phase of current density is antisymmetrically distributed along the  $z$  direction, as shown in Figs. 6(a) and 6(b).

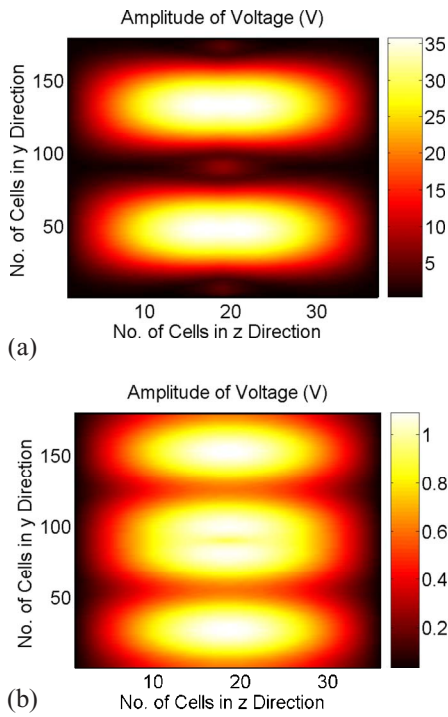


FIG. 4. (Color online) The voltage-amplitude distributions of guided waves propagating in the waveguides when  $d=5$  mm and TL meshes are terminated by the wave impedance of free space. (a) The super waveguide with  $\delta=-0.0085$ . (b) The conventional RHTL waveguide.

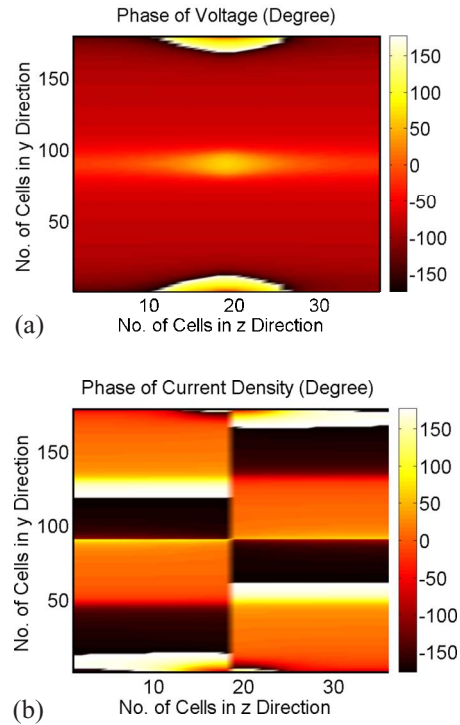


FIG. 6. (Color online) The phase distributions of guided waves propagating in the super waveguide when  $d=5$  mm and TL meshes are terminated by the wave impedance of free space. (a) Voltage. (b) Current density.

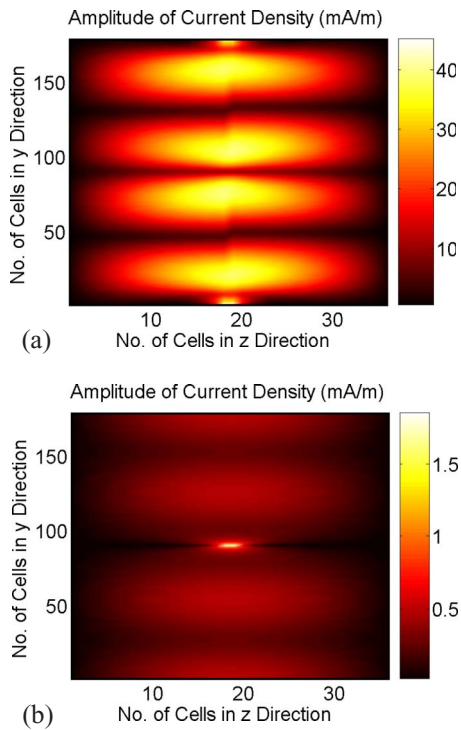


FIG. 5. (Color online) The current-density amplitude distributions of guided waves propagating in the waveguides when  $d=5$  mm and TL meshes are terminated by the wave impedance of free space. (a) The super waveguide with  $\delta=-0.0085$ . (b) The conventional RHTL waveguide.

The power-density distributions excited by the point voltage source in such two waveguides are demonstrated in Fig. 7. In the conventional RHTL waveguide, the power density is symmetrically distributed along the  $z$  direction and anti-symmetrically distributed along the  $y$  direction, as shown in Fig. 7(b). The antisymmetry implies that the power density is guided along the  $+y$  direction above the source point and  $-y$  direction below the source point. We remark that the power densities around the source point (in the center of the figure) has been suppressed to a maximum value of  $0.55$  mW/m to observe the up-going and down-going waves clearly. In the RHTL-LHTL super waveguide, however, the power density is antisymmetrically distributed along both  $y$  and  $z$  directions, as shown in Fig. 7(a), indicating the power to be guided along opposite directions in the RHTL and LHTL regions. This is exactly the same as the theoretical analysis [8,9].

From Fig. 7, we observe that the maximum power density guided along the super waveguide is  $200$  mW/m, and the maximum power density guided along the conventional waveguide is  $0.55$  mW/m under the same excitation. Hence the power density generated and transmitted in the super waveguide is about 364 times larger than that in the conventional waveguide. Such high-power density generation and transmission in the super waveguide do not violate the energy conservation since the power flows in the RHTL and LHTL regions are in opposite directions. After simple calculation, the total power flowing across the RHTL region towards the  $+y$  direction is  $127.3$  mW, while the total power flowing across the LHTL region towards the  $-y$  direction is

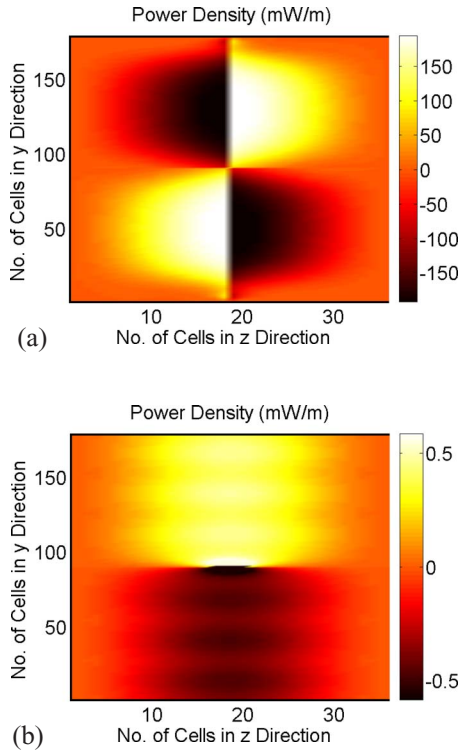


FIG. 7. (Color online) The power-density distributions of the guided waves propagating in the waveguides when  $d=5$  mm and TL meshes are terminated by the wave impedance of free space. (a) The super waveguide with  $\delta=-0.0085$ . (b) The conventional RHTL waveguide.

$-126.8$  mW. Hence the net power flow towards the  $+y$  direction across the whole waveguide is  $0.5$  mW, which is nearly the same as that in the conventional RHTL waveguide. That is to say, high-power flows are generated and transmitted in both RHTL and LH TL regions with opposite directions.

We have also studied the lossy effect of LHM to the high-power density generation and transmission. When we choose  $\delta=-0.0085$  and  $\sigma_\mu=\sigma_\epsilon=0.001$ , the power-density distribution of the guided wave propagating in the lossy super waveguide is quite similar to that shown in Fig. 7(a). The only difference is, the maximum value of the power density reduces to  $192$  mW/m. When we further increase the loss to  $\sigma_\mu=\sigma_\epsilon=0.01$ , the maximum power density reduces to  $115$  mW/m. Clearly, even though a moderate loss of  $0.01$  is involved in LH TL, the transmitted power density is still  $209$  times larger than that in the conventional waveguide.

In the above simulation results, a total of  $36 \times 180$  unit cells have been used ( $d=5$  mm) with the source located at node  $(9, 90)$  for the RHTL-LH TL super waveguide. As a result, the observation region along the  $y$  direction is only  $1.5\lambda_0$  ( $\lambda_0$  is the wavelength in free space). In such a case, the super-waveguide phenomenon may be produced by the near-field effect or resonance. Hence it is necessary to investigate the field-transmission property in a long range.

To make a long-range super waveguide in the  $y$  direction, we use  $18$  unit cells along the  $z$  direction due to the memory limit in ADS, in which  $9$  cells are for RHTL and  $9$  cells for LH TL. A total of  $700$  unit cells are used in the  $y$  direction,

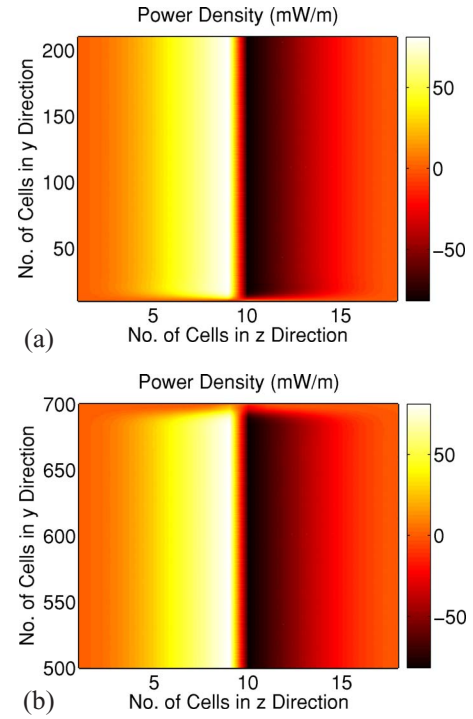


FIG. 8. (Color online) The power-density distributions of the guided wave propagating in long-range super waveguide when  $d=1$  cm,  $\delta=-0.01$ , and TL meshes are terminated by the wave impedance of free space. (a) Near-field region (from  $0.33\lambda_0$  to  $7\lambda_0$ ). (b) Far-field region (from  $16.33\lambda_0$  to  $23.3\lambda_0$ ).

which is  $23.3\lambda_0$  long. Here, the size of unit cell is set as  $d=1$  cm to meet the guidance condition. The voltage source is placed at node  $(4, 10)$  in the RHTL region to have a longer observation range above the source. The retardation parameters are set as  $\delta=0.01$  and  $\sigma_\mu=\sigma_\epsilon=0$ .

Figure 8 illustrates the simulation results of power densities on the long waveguide, in which Fig. 8(a) shows the power-density distributions from unit  $10$  to unit  $210$  ( $0.33\lambda_0$  to  $7\lambda_0$ ) along the  $y$  direction and Fig. 8(b) shows the power densities from unit  $500$  to unit  $700$  ( $16.33\lambda_0$  to  $23.3\lambda_0$ ). From Fig. 8, we clearly observe that the maximum power density is  $80.5$  mW/m, which is  $146$  times higher than that in the conventional RHTL waveguide. Similarly to Fig. 7, high power flows are transmitted in both RHTL and LH TL regions with opposite directions. We also notice that the high-power densities can propagate in a long range, from near-field region to far-field region, without attenuation. Hence the super waveguide phenomenon still exists even when the waveguide is very long.

We remark that the decrease of the maximum power density shown in Fig. 8 versus that in Fig. 7(a) is due to the larger unit cell ( $d=1$  cm), which causes larger spatial dispersion, and the larger retardation parameter ( $\delta=0.01$ ).

To demonstrate the above conclusions, we make a rigorous analysis of the energy speeds in both RHTL and LH TL regions. In the equivalent medium model of the RHTL-LH TL waveguide shown in Fig. 2(b), the dispersion equation is given by

$$k_{mz}^2 + k_y^2 = \omega^2 \mu_m \epsilon_m, \quad (8)$$

where  $m=0$  represents the RHTL region and  $m=1$  represents the LHTL region. Due to the field distributions shown in Figs. 3, 4, and 8, the electric field in the far-field region to the source can be expressed as

$$E_{0x} = \sin(k_{0z}z)e^{ik_y y}, \quad E_{1x} = \sin[k_{1z}(z-a)]e^{ik_y y}, \quad (9)$$

in which  $a$  is the width of super waveguide. Based on the boundary condition at  $z=a/2$ , we then have  $k_{0z} = -k_{1z}$ , which is exactly the same as the theoretical analysis in Ref. [8]. From Figs. 3, 4, and 8, we notice that only the dominant mode exists. Hence we can choose  $k_{0z} = -k_{1z} = \pi/a$  [8]. From the Maxwell's equations, the magnetic field is written as

$$H_{my} = \frac{1}{i\omega\mu_m} \frac{\partial E_{mx}}{\partial z}, \quad H_{mz} = -\frac{k_y}{\omega\mu_m} E_{mx}. \quad (10)$$

Furthermore, we get the power densities along the  $y$  direction using the Poynting's theorem as

$$S_{0y} = \frac{k_y}{\omega\mu_0} \sin^2(k_{0z}z), \quad S_{1y} = \frac{k_y}{\omega\mu_1} \sin^2[k_{1z}(z-a)]. \quad (11)$$

The energy velocity  $v_e$  is defined as the ratio of the integral Poynting vector to the total energy. Hence we have the energy velocities in both RHTL and LHTL parts as

$$v_{e0} = \int_0^{a/2} S_{0y} dz \Big/ \int_0^{a/2} (w_{e0} + w_{m0}) dz, \quad (12)$$

$$v_{e1} = \int_{a/2}^a S_{1y} dz \Big/ \int_{a/2}^a (w_{e1} + w_{m1}) dz, \quad (13)$$

in which  $w_{e0}$ ,  $w_{m0}$ ,  $w_{e1}$ , and  $w_{m1}$  are electric and magnetic energy densities in the RHTL and LHTL regions, respectively. When we choose  $f=1$  GHz and  $d=1$  cm, the energy velocities in the RHTL and LHTL regions are computed as  $1.6583 \times 10^8$  m/s and  $-1.6583 \times 10^8$  m/s, respectively. This is consistent with the simulation results shown in Figs. 7 and 8.

#### IV. CONCLUSIONS

We have realized the super waveguide for high-power density generation and transmission using the RHTL-LHTL circuits. Through accurate ADS simulations, we show that high-power flows with opposite directions are excited in the RHTL and LHTL regions of the super waveguide, which form the energy vortices in the waveguide cross section. Rigorous analysis of the energy velocities in the RHTL and LHTL regions validates the conclusions.

#### ACKNOWLEDGMENTS

This work was supported in part by the National Science Foundation of China under Grant Nos. 60671015, 60496317, 60225001, and 60621002, in part by the National Basic Research Program (973) of China under Grant No. 2004CB719802, and in part by the National Doctoral Foundation of China under Grant No. 20040286010. D.R.S. acknowledges support from the Air Force Office of Scientific Research through a Multiple University Research Initiative, Contract No. FA9550-06-1-0279.

[1] V. G. Vesalago, *Sov. Phys. Usp.* **10**, 509 (1968).  
 [2] N. Engheta, *IEEE Antennas Propag. Mag.* **1**, 10 (2002).  
 [3] I. S. Nefedov and S. A. Tretyakov, *Radio Sci.* **38**, 1101 (2003).  
 [4] B. I. Wu, T. M. Grzegorzczak, Y. Zhang, and J. A. Kong, *J. Appl. Phys.* **93**, 9386 (2003).  
 [5] D. K. Qing and G. Chen, *Appl. Phys. Lett.* **84**, 669 (2004).  
 [6] L. Shen, S. He, and S. Xiao, *Phys. Rev. B* **69**, 115111 (2004).  
 [7] G. D'Aguzzo, N. Mattiucci, M. Scalora, and M. J. Bloemer, *Phys. Rev. E* **71**, 046603 (2005).  
 [8] Q. Cheng and T. J. Cui, *Phys. Rev. B* **72**, 113112 (2005).  
 [9] Q. Cheng and T. J. Cui, *Opt. Express* **13**, 10230 (2005).

[10] J. F. Zhang and T. J. Cui, *IEEE Trans. Antennas Propag.* **54**, 9 (2006).  
 [11] R. A. Shelby, D. R. Smith, and S. Schultz, *Science* **292**, 77 (2001).  
 [12] D. Schurig, J. J. Mock, and D. R. Smith, *Appl. Phys. Lett.* **88**, 041109 (2005).  
 [13] A. Grbic and G. V. Eleftheriades, *Phys. Rev. Lett.* **92**, 117403 (2004).  
 [14] T. J. Cui, Q. Cheng, Z. Z. Huang, and Y. J. Feng, *Phys. Rev. B* **72**, 035112 (2005).